Oxidic Nanorods

G. R. Patzke, F. Krumeich, R. Nesper,
Angew. Chem. Int.Ed. Engl. 14 (2002) 2447

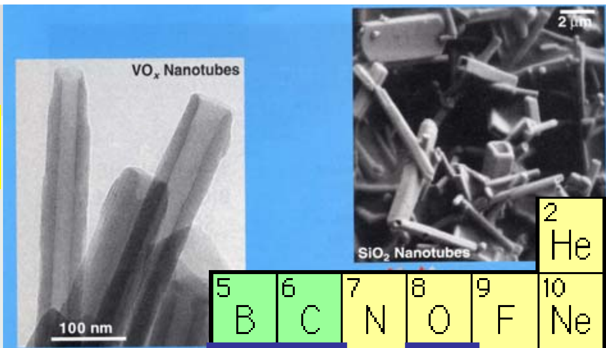

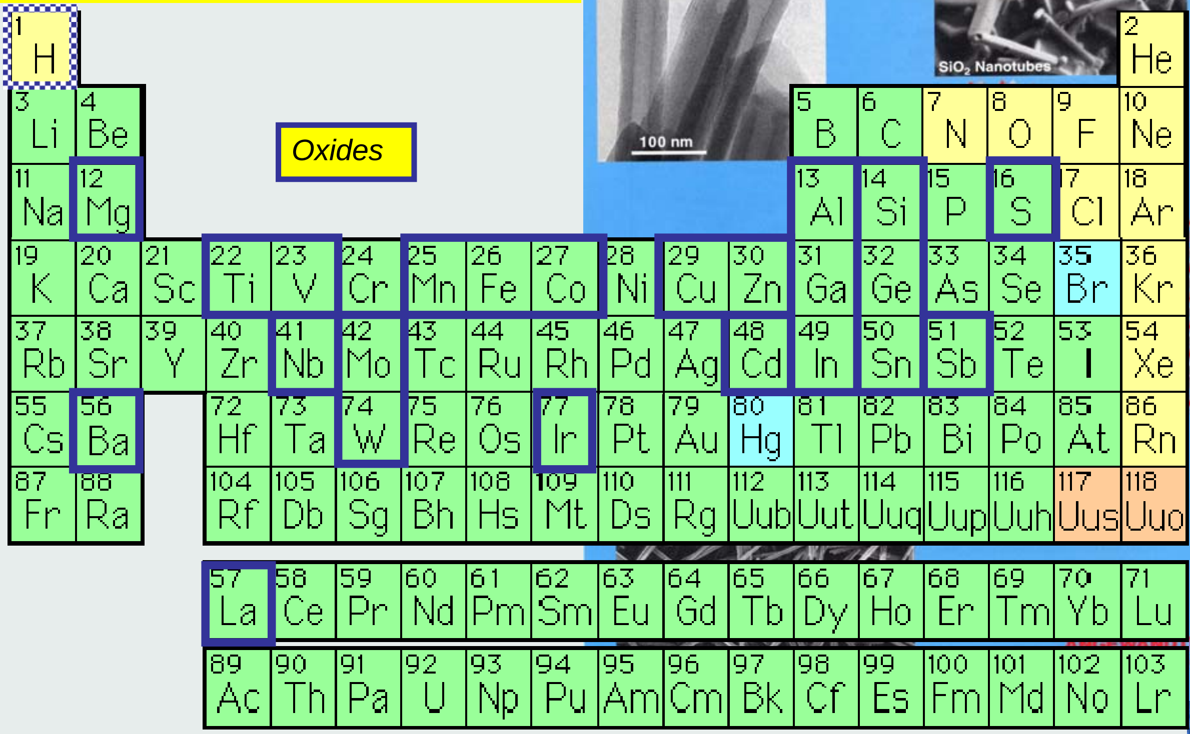

Rods, Fibers, Filaments

Table 1. Synthetic routes for oxidic nanorods (published since 1995).

Oxide	Synthetic route	Ref.	Oxide	Synthetic route	Ref.
$BaCrO_4$	Fusion of reverse micelles and microemulsion droplets	[122]	MnO_2	Template method with alumina membranes	[127]
$BaSO_4$	Precipitation from aqueous solution in presence of polymers	[123]	MnO_2	Hydrothermal synthesis	[142]
$BaWO_4$	Reversed micelle templating method	[124]	MoO_3	Template-directed reaction of molybdic acid and subsequent leaching process	[143]
CdO	Evaporation of metal oxide powders at high temperatures	[125]	MoO_3	Templating against carbon nanotubes	[65]
$CdWO_4$	Hydrothermal treatment of $CdCl_2$ and Na_2WO_4	[126]	MoO_2	Templating against carbon nanotubes	[65]
Co_3O_4	Template method with alumina membranes	[127]	$PbTiO_3$	Sol-gel electrophoresis, deposition in polycarbonate membrane	[144]
CuO	Room temperature reaction of $CuCl_2 \cdot 2H_2O$ and NaOH with PEG 400	[128]	RuO_2	Templating against carbon nanotubes	[65]
Fe_2O_3	Thin-film processing method	[129]	Sb_2O_3	Microemulsion method for the system AOT–water–toluene[a]	[145]
Fe_3O_4	Sonication of aqueous iron(II) acetate in the presence of β-cyclodextrin	[130]	Sb_2O_5	Microemulsion method for the system AOT–water–toluene[a]	[145]
Ga_2O_3	DC arc discharge of GaN powders in Ar/O_2 mixture	[131]	Sb_2O_5	Templating against carbon nanotubes	[65]
Ga_2O_3	Gas reaction method starting from Ga and O_2 at 780 °C	[132]	SnO_2	Annealing of powders generated from inverse microemulsions	[146]
Ga_2O_3	Physical evaporation at 300 °C from a bulk gallium target	[133]	SnO_2	Evaporation of metal oxide powders at high temperatures	[125]
Ga_2O_3	DC arc discharge (GaN, graphite, nickel powder)	[134]	SiO_2	Helical mesostructured tubules from Vortex-Assisted Surfactant Templates	[147]
Ga_2O_3	Electric arc discharge of GaN powders mixed with Ni and Co	[135]	TiO_2	Sol-gel template method employing alumina membranes	[148]
Ga_2O_3	Heating of Ga with SiO_2 powder and a Fe_2O_3 catalyst	[136]	V_2O_5	Vanadium pentoxide gels	[149]
GeO_2	Carbon-nanotube confined reaction of metallic Ge	[137]	V_2O_5	Templating against carbon nanotubes	[65]
In_2O_3	Evaporation of metal oxide powders at high temperatures	[125]	WO_3	Templating against carbon nanotubes	[65]
In_2O_3	Growth from Au droplets	[138]	YBCO	Laser ablation of a high T_c superconductor $YBa_2Cu_3O_7$	[150]
IrO_2	Templating against carbon nanotubes	[65]	ZnO	Gas reaction employing Zn and H_2O	[151]
$K_2Ti_6O_{13}$	Calcination of KF and TiO_2	[139]	ZnO	Evaporation of metal oxide powders at high temperatures	[125]
MgO	Vapor-solid growth process with in situ generated Mg vapor	[114]	ZnO	Catalyzed epitaxial growth	[152]
MgO	Heating of $MgCl_2$ at 750 °C in mixture gas (Ar/H_2) ■■not O_2? ■■	[140]	ZnO	Self-organization of nanoparticles	[153]
$Mg(OH)_2$	Solvothermal treatment of Mg, H_2O, and ethylenediamine	[141]			

G. Patzke, F. Krumeich, R. Nesper, Angew. Chem. 2002, 114, 2554

Anisotropic Particles

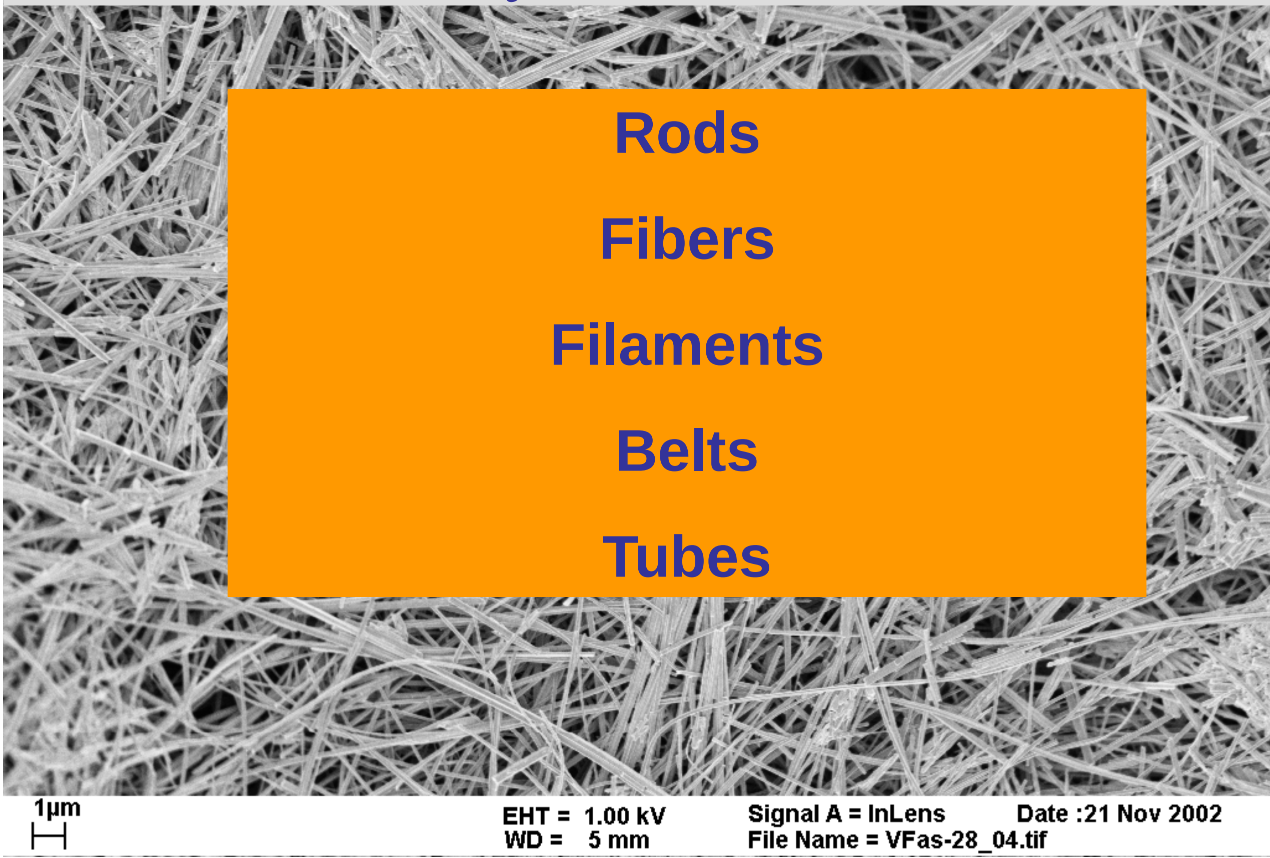

Rods

Fibers

Filaments

Belts

Tubes

Growth Conditions

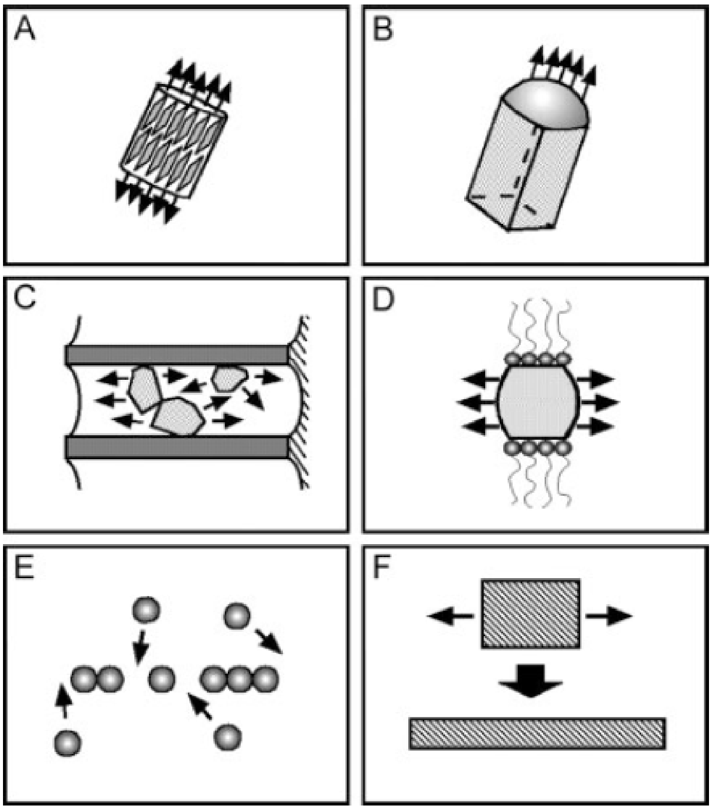

Fig. 1. Schematic illustrations of six different strategies that have been demonstrated for achieving 1D growth: a) dictation by the anisotropic crystallographic structure of a solid; B) confinement by a liquid droplet as in the vapor–liquid–solid process; C) direction through the use of a template; D) kinetic control provided by a capping reagent; E) self-assembly of 0D nanostructures; and F) size reduction of a 1D microstructure.

Phase Segregation

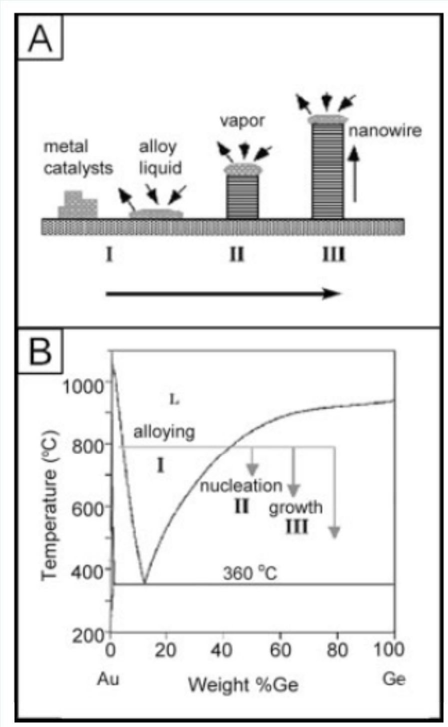

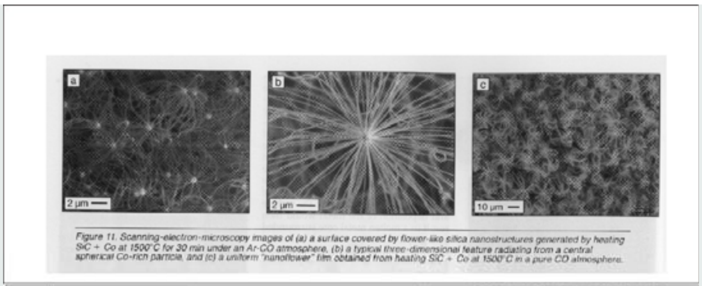

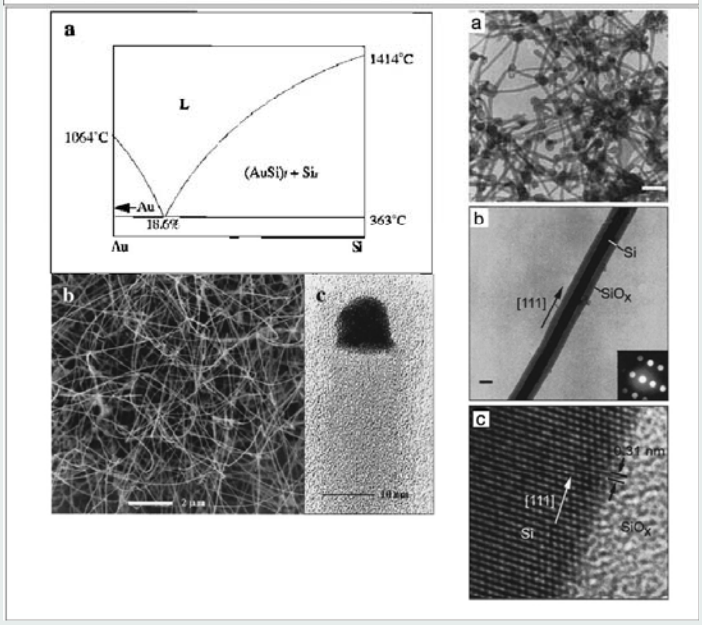

Surface Structures as Templates

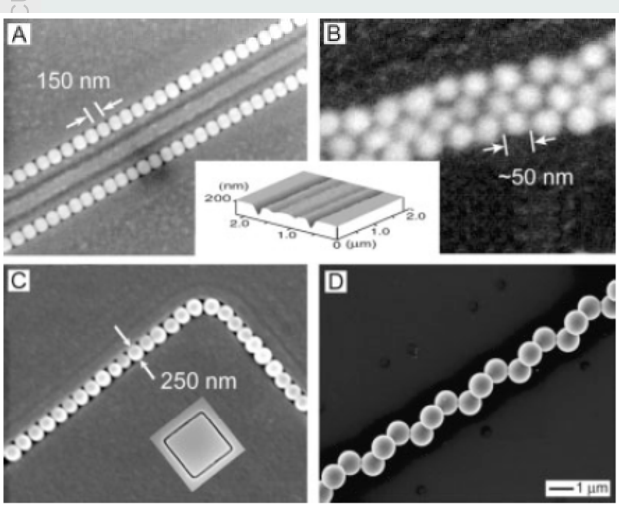

Fig. 21. A,B) Structures that were assembled from 150 nm polystyrene beads (A), and 50 nm Au colloids (B), by templating against 120 nm-wide channels patterned in a thin photoresist film (see the inset) [161a]. C) An L-shaped chain of Au@SiO_2 spheres assembled against a template (see the inset) patterned in a thin photoresist film [161c]. D) A spiral chain of polystyrene beads that were assembled by templating against a V-groove etched in the surface of a Si(100) wafer [161d].

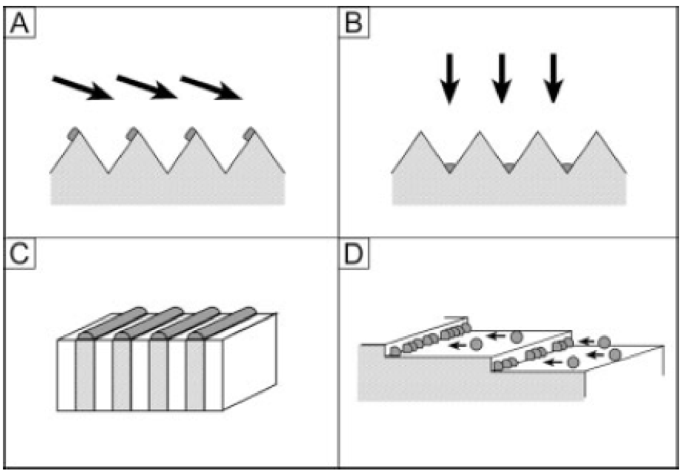

Fig. 6. Schematic illustrations of procedures that generated 1D nanostructures by A) shadow evaporation [58]; B) reconstruction at the bottom of V-grooves [60]; C) cleaved-edge overgrowth on the cross-section of a multilayer film [64]; and D) templating against step edges on the surface of a solid substrate [68].

Semiconductors

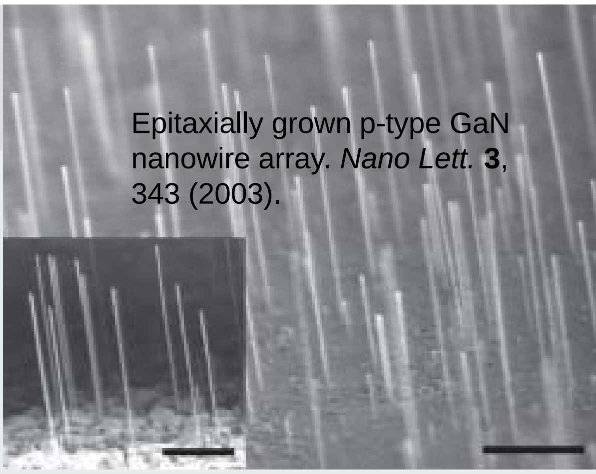

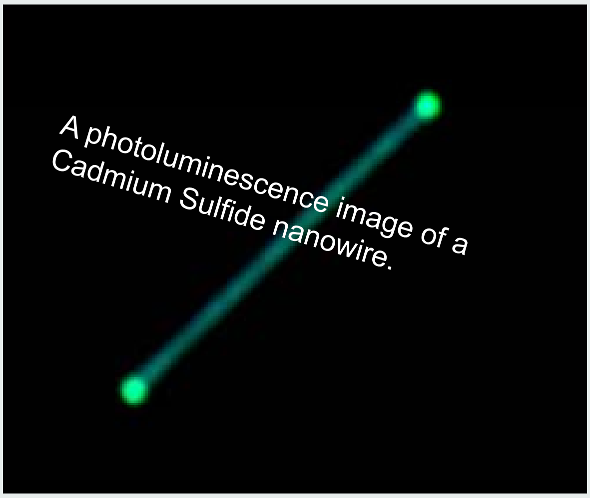

Photoluminescence

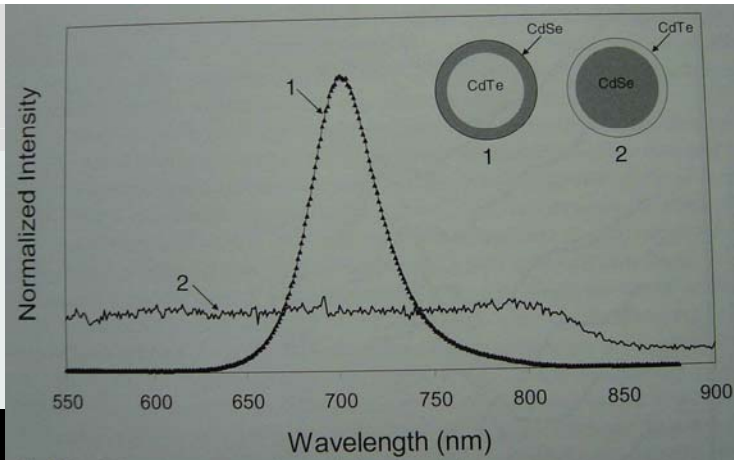

Fig. 12.1. Schematic structures of core–shell semiconductor nanocrystals and corresponding photoluminescence spectra.

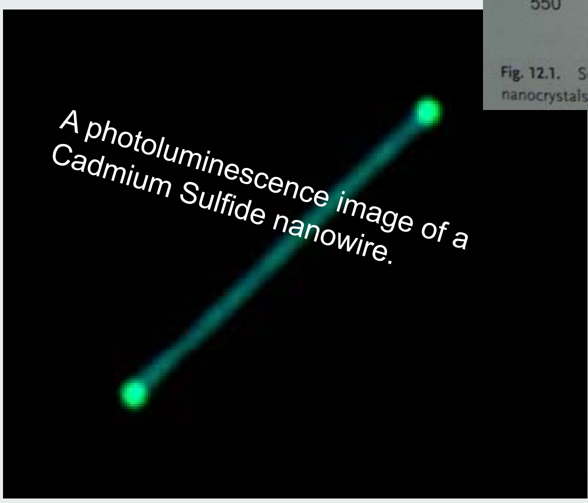

gold-tipped CdSe nanorods

Directed self-assembly of gold-tipped CdSe nanorods
Asaf Salant, Ella Amitay-Sadovsky, Uri Banin
J. AM. CHEM. SOC. 2006, 128, 10006-10007

Scheme 1. Reacting Biotin Disulfide (Green) with NDBs and Avidin (Orange) Using Different Mole Ratios, Resulting in Dimers, Flowers, and Trimers

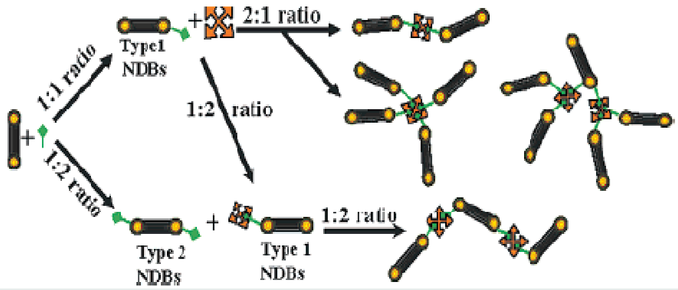

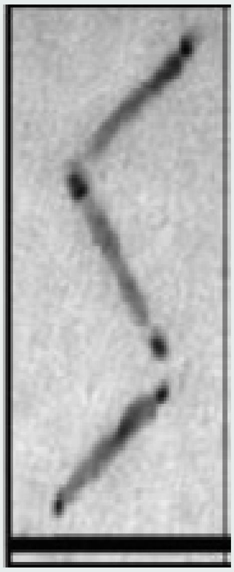

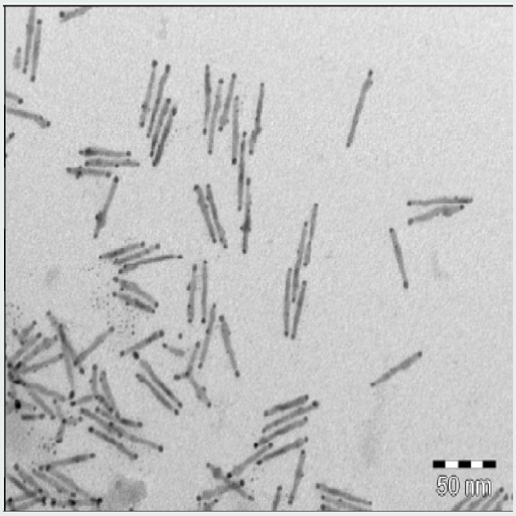

Gold-tipped CdSe nanorods

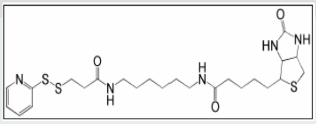

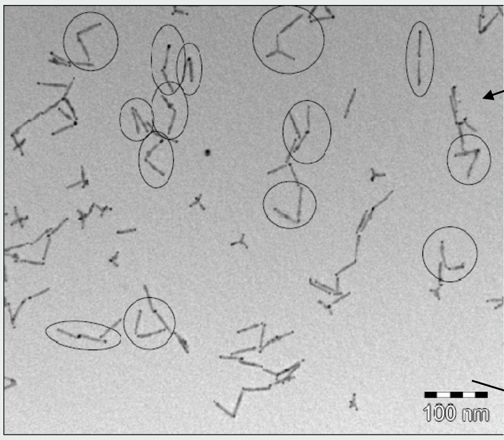

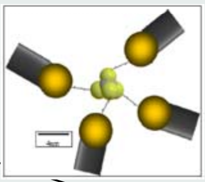

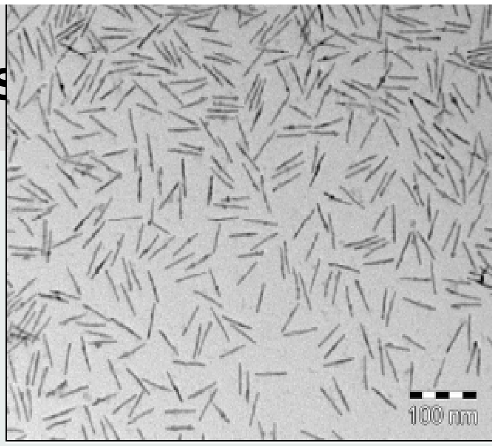

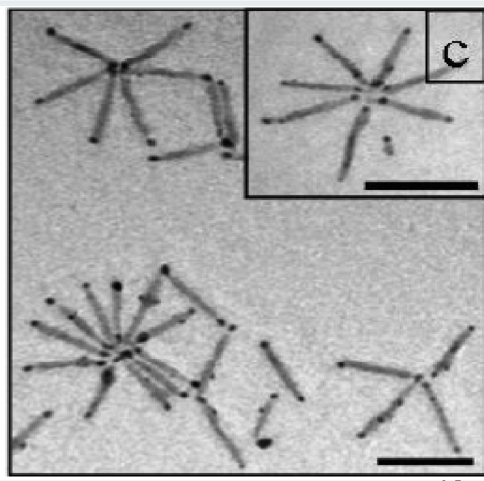

CdSe nanorods were reacted as the dimer scheme, show mostly of side-to-side interactions.

Nanofibers by Crystal Structure

Selenium

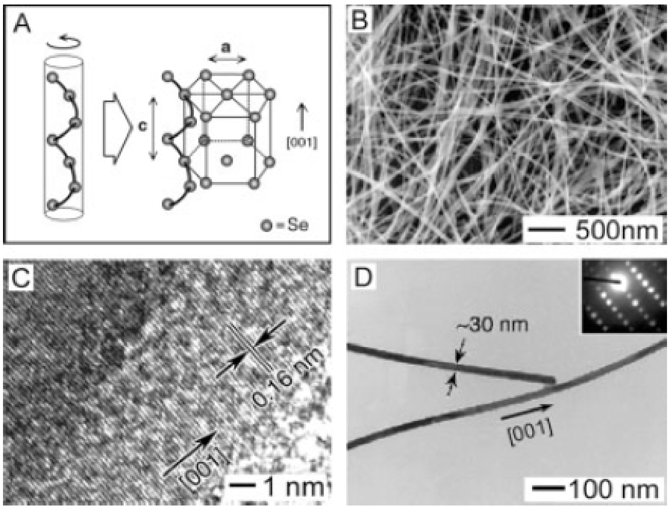

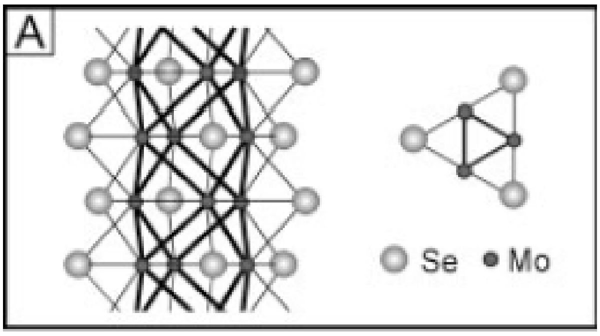

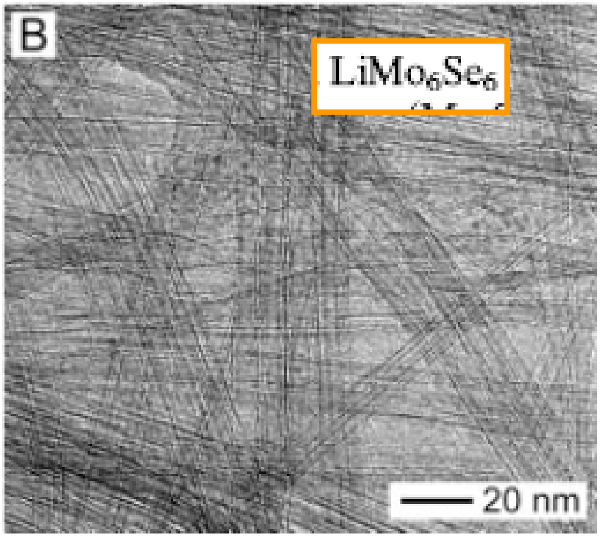

SnO_2 NRs – Growth Mechanism

Synthesis and Characterization of Rutile SnO_2 Nanorods**

By *Yingkai Liu,** *Changlin Zheng, Wenzhong Wang, Chunrong Yin,* and *Guanghou Wang*

Adv. Mater. **2001**, *13*, No. 24, December 17

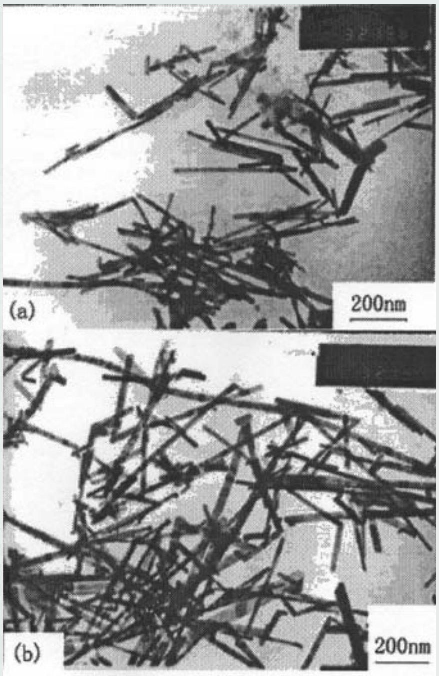

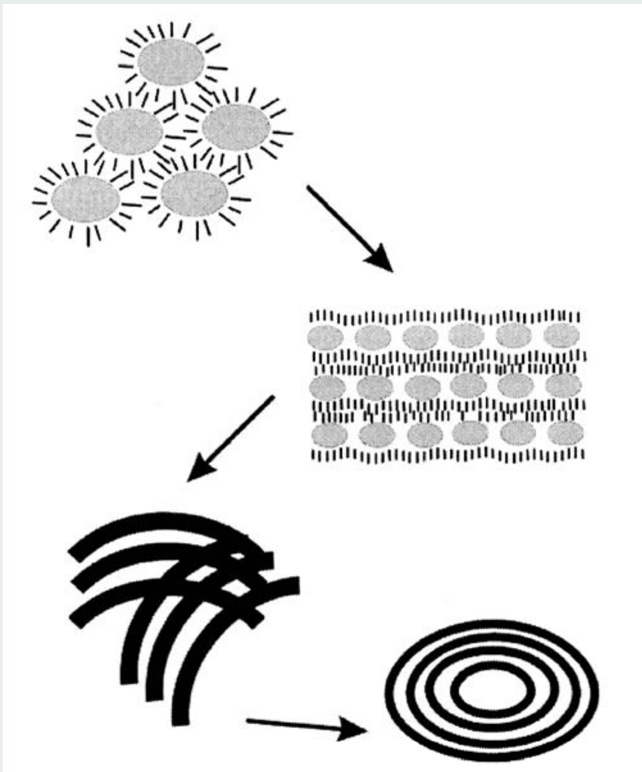

Alumina Membranes as Outer Templates

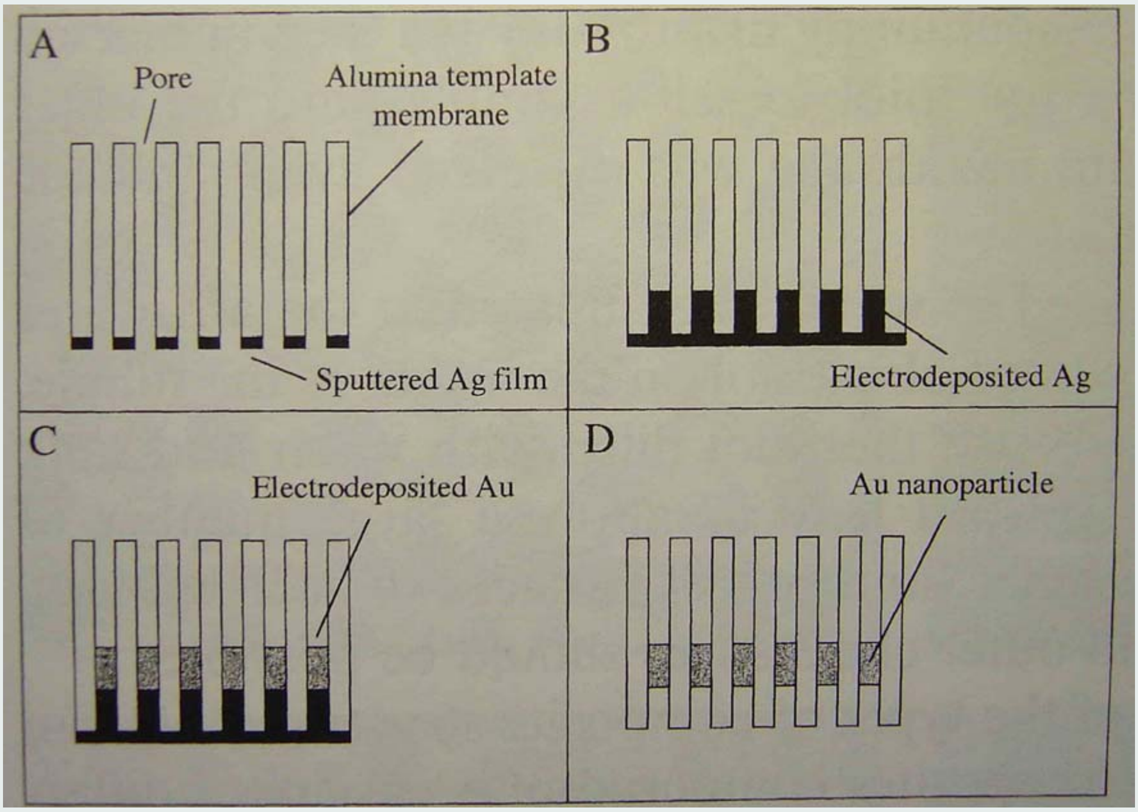

Alumina Membranes as Outer Templates

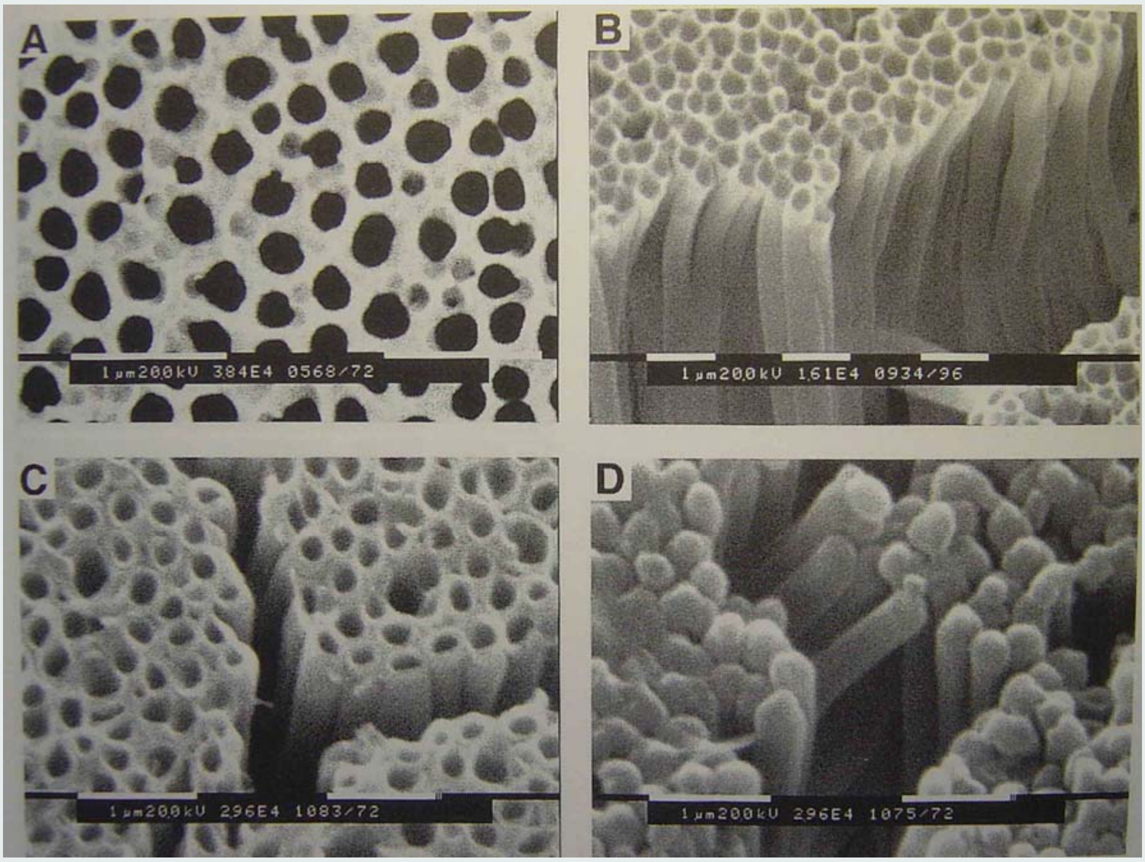

Hetero-Structured Nano Wires

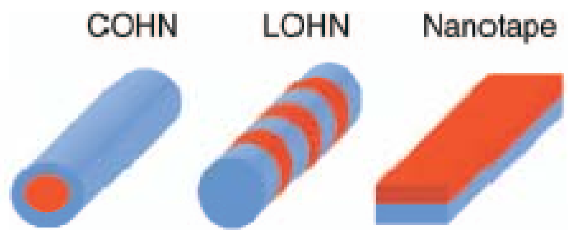

Figure 3. Three different types of heterostructured nanowires: a coaxial heterostructured nanowire (COHN), a longitudinal heterostructured nanowire (LOHN), and a nanotape.

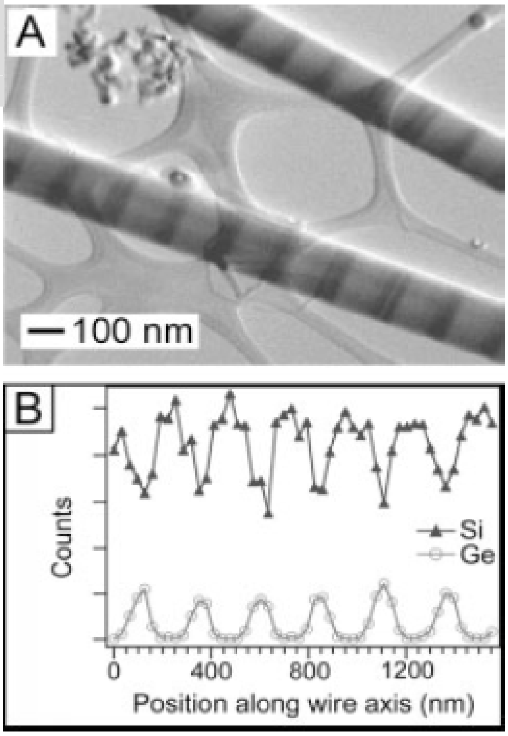

Fig. 23. A) A TEM image of two typical Si/SiGe superlattice nanowires. B) Compositional profiles showing the spatial modulation in Si and Ge contents along the longitudinal axis of a nanowire [186].

Detailed models of phonon heat conduction in semiconducting nanowires that consider modified dispersion relations and all-important scattering processes predict a large decrease (90%) in the lattice thermal conductivity of wires tens of nanometers in diameter.

Peidong Yang
MRS BULLETIN
VOLUME 30, 2005